SFB/CPP-08-56
TTP08-34

Fermionic contributions to the three-loop static potential

Alexander V. Smirnov[(a,c)], Vladimir A. Smirnov[(b,c)], Matthias Steinhauser[(c)]

(a) Scientific Research Computing Center, Moscow State University
119992 Moscow, Russia
(b) Nuclear Physics Institute, Moscow State University
119992 Moscow, Russia
(c) Institut für Theoretische Teilchenphysik, Universität Karlsruhe (TH)
Karlsruhe Institute of Technology (KIT)
76128 Karlsruhe, Germany

Abstract

We consider the three-loop corrections to the static potential which are induced by a closed fermion loop. For the reduction of the occurring integrals a combination of the Gröbner and Laporta algorithm has been used and the evaluation of the master integrals has been performed with the help of the Mellin-Barnes technique. The fermionic three-loop corrections amount to 2% of the tree-level result for top quarks, 8% for bottom quarks and 27% for the charm quark system.

PACS numbers: 12.38.Bx, 14.65.Dw, 14.65.Fy, 14.65.Ha

1 Introduction

The potential between a heavy quark and its anti-quark is a crucial quantity both for understanding fundamental properties of QCD, such as confinement, and for describing the rich phenomenology of heavy quarkonia [1] (see also Ref. [2] for a recent review about the static potential).

Within perturbation theory the static potential can be computed as an expansion in the strong coupling α_s and the inverse heavy-quark mass or, equivalently, in the heavy-quark velocity v. The leading order result in v is known up to the two-loop approximation [3–8] which has been completed about ten years ago. For the three-loop corrections there are only estimates relying on Padé approximations [9] or based on renormalon studies [10].

A new feature of the three-loop corrections is the appearance of an infrared divergence which was discussed for the first time in Ref. [11]. A quantitative analysis of this effect can be found in Ref. [12] (see also Ref. [13]) where a proper definition of the static potential within perturbation theory is provided. Furthermore, it is argued that the infrared singularities cancel in physical quantities after including the contribution where so-called ultra-soft gluons interact with the heavy quark anti-quark bound state (see also, e.g., Refs. [14–16]). Higher order logarithmic contributions to the infrared behaviour of the static potential have been considered in Refs. [17, 18].

In this paper we compute the fermionic contribution to the three-loop static potential which is infrared safe. Partial results have already been published in Refs. [19, 20].

The static potential enters as a building block in a variety of physical quantities. Often at three-loop order only estimations are used or the three-loop coefficient — usually called a_3 — appears as a parameter in the final result. Let us in this context mention the determination of the bottom and top quark mass from the ground state energy of the heavy quark system which has been computed to third order in Ref. [16]. The error on the mass values due to the unknown three-loop coefficient amounts to 14% (13%) of the total uncertainty for the bottom (top) quark. Similarly, a_3 enters the calculation of the total cross section for top quark threshold production at next-to-next-to-next-to leading order (see, e.g., Ref. [21]). The static energy between two heavy quarks has often been used in order to compare perturbative calculations with simulations on the lattice (see, e.g., Refs. [22–25]). Also in this context the knowledge of a_3 is crucial and is expected to lead to a better agreement between the two approaches [24]. Last not least let us mention the extraction of the strong coupling from lattice simulations where again the static potential plays a crucial role [26, 27] and the knowledge of a_3 would be highly desirable.

Let us for completeness mention that the one-loop mass-suppressed corrections to the static potential have been evaluated in Refs. [28–33], the two-loop terms in Ref. [8]. Light quark mass effects have been considered in Ref. [34]. A collection of all relevant contributions needed up to next-to-next-to-next-to-leading order can be found in Ref. [15]. Furthermore, the two-loop corrections for the case where the quark and anti-quark form

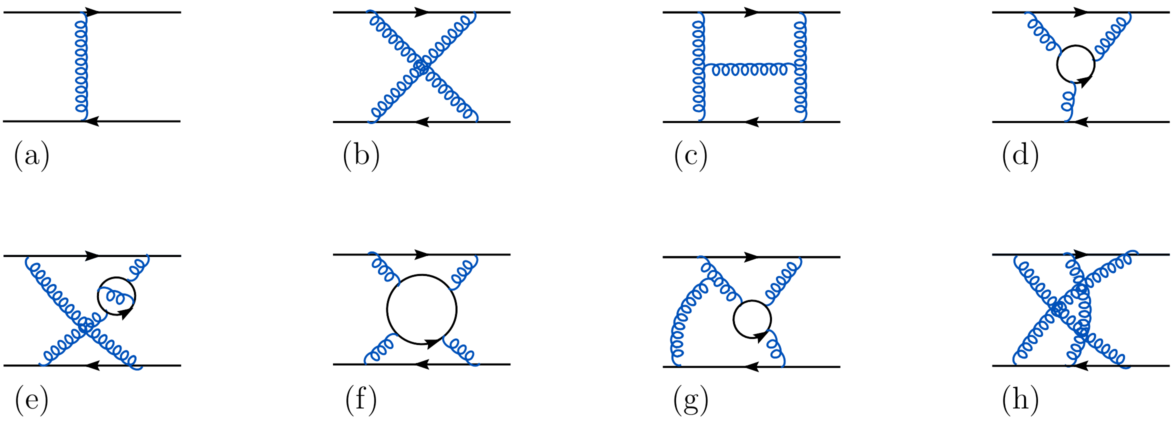

Figure 1: Sample diagrams contributing to the static potential at tree-level, one-, two- and three-loop order. In this paper only the fermionic corrections are considered at three-loop order which excludes diagrams of type (h).

an octet state have been evaluated in Ref. [35].

The remainder of the paper is organized as follows: In the next Section we present details of our calculation. In particular we discuss the various types of Feynman diagrams which occur at three-loop order and their contributions to the individual colour factors. In Section 3 our results are presented and Section 4 contains our conclusions.

2 Calculation

In the practical calculation of quantum corrections to the static potential one has to consider a heavy quark and its anti-quark which interact via the exchange of gluons. In Fig. 1 some sample diagrams up to three-loop order are shown.

In momentum space the static potential can be cast into the form

$$V(|\vec{q}\,|) = -\frac{4\pi C_F \alpha_s(|\vec{q}\,|)}{\vec{q}^{\,2}} \left[1 + \frac{\alpha_s(|\vec{q}\,|)}{4\pi} a_1 + \left(\frac{\alpha_s(|\vec{q}\,|)}{4\pi}\right)^2 a_2 + \left(\frac{\alpha_s(|\vec{q}\,|)}{4\pi}\right)^3 \left(a_3 + 8\pi^2 C_A^3 \ln\frac{\mu^2}{\vec{q}^{\,2}} \right) + \cdots \right], \tag{1}$$

where α_s denotes the strong coupling in the $\overline{\mathrm{MS}}$ scheme and explicit results for a_1 [3, 4] and a_2 [5–8] are given below in Eq. (4). The infrared logarithm at order α_s^3 follows the conventions of Ref. [15] and the renormalization group logarithms $\ln(\mu^2/\vec{q}^{\,2})$ can be recovered with the help of

$$
\begin{aligned}
\frac{\alpha_s(|\vec{q}\,|)}{\pi} &= \frac{\alpha_s(\mu)}{\pi}\Bigg[1+\frac{\alpha_s(\mu)}{\pi}\beta_0 L+\left(\frac{\alpha_s(\mu)}{\pi}\right)^2 L\left(\beta_0^2 L+\beta_1\right) \\
&\quad +\left(\frac{\alpha_s(\mu)}{\pi}\right)^3 L\left(\beta_0^3 L^2+\frac{5}{2}\beta_0\beta_1 L+\beta_2\right)+\cdots\Bigg]\,, \qquad (2)
\end{aligned}
$$

where $L=\ln(\mu^2/\vec{q}^{\,2})$ and the coefficients of the β function (see, e.g., Ref. [36]) read

$$
\begin{aligned}
\beta_0 &= \frac{1}{4}\left(\frac{11}{3}C_A-\frac{4}{3}T_F n_l\right)\,, \\
\beta_1 &= \frac{1}{16}\left(\frac{34}{3}C_A^2-\frac{20}{3}C_A T_F n_l-4C_F T_F n_l\right)\,, \\
\beta_2 &= \frac{1}{64}\Bigg(\frac{2857}{54}C_A^3-\frac{1415}{27}C_A^2 T_F n_l-\frac{205}{9}C_A C_F T_F n_l+2C_F^2 T_F n_l+\frac{158}{27}C_A T_F^2 n_l^2 \\
&\quad +\frac{44}{9}C_F T_F^2 n_l^2\Bigg)\,. \qquad (3)
\end{aligned}
$$

Here, $C_A=N_c$ and $C_F=(N_c^2-1)/(2N_c)$ are the eigenvalues of the quadratic Casimir operators of the adjoint and fundamental representations of the $SU(N_c)$ colour gauge group, respectively, $T_F=1/2$ is the index of the fundamental representation, and n_l is the number of light-quark flavours. Let us at this point only mention that a_1 has the colour structures C_A and $T_F n_l$ where the latter contribution originates from one-loop fermionic corrections to the gluon propagator. Note that there is no colour factor C_F since this contribution is generated via an iteration of the tree-level result. Consider, e.g., the one-loop planar-ladder and the crossed-ladder diagram of Fig. 1(b) with the colour factors C_F^2 and $C_F^2-C_AC_F/2$, respectively. It is easy to see (see, e.g., Ref. [37]) that the C_F^2 term can be generated by iterations of the leading order diagram in Fig. 1(a) leaving only the C_AC_F term as genuine one-loop contribution.

Similarly, at two-loop order there are the colour factors C_A^2, $C_AT_Fn_l$, $C_FT_Fn_l$, and $(T_Fn_l)^2$ where the latter two originate from loop corrections to the gluon propagator connecting the quark and the anti-quark. a_2 contains no C_F^2 and C_FC_A terms since their contribution is again generated by iterations of lower-order results.

The rule that a colour factor C_F can only arise from corrections to a fermion bubble in a gluon line also holds at three-loop level. This requires a careful analysis of the colour factors for each class of diagram. For example, the colour factor of the graph in Fig. 1(e) receives a contribution[1] $(C_F-C_A/2)T_Fn_l$ from two-loop fermionic subdiagram and a factor $(C_F-C_A/2)$ from the remaining crossed box structure. Whereas the complete first factor has to be taken into account only the C_A term of the second factor contributes to the potential. In a similar manner all diagrams have to be analyzed which leads to the colour

[1] In addition to the factor C_F already present in Eq. (1).

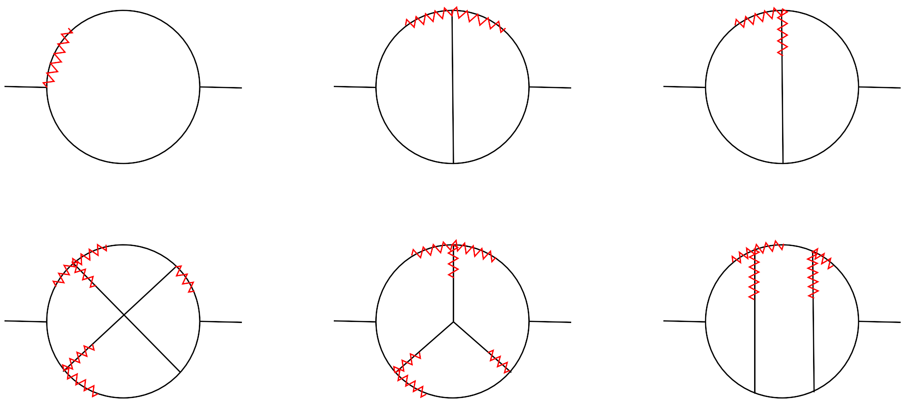

Figure 2: One-, two- and three-loop diagrams. The solid line stands for massless relativistic propagators and the zigzag line represents static propagators.

structures C_A^3, $C_A^2 T_F n_l$, $C_A C_F T_F n_l$, $C_F^2 T_F n_l$, $C_A (T_F n_l)^2$, $C_F (T_F n_l)^2$ and $(T_F n_l)^3$. In this paper we compute all coefficients except the one of C_A^3. The results for the structures $C_A (T_F n_l)^2$, $C_F (T_F n_l)^2$ and $(T_F n_l)^3$ can be found in Refs. [19, 20].

At three-loop order there is a new class of diagrams containing a "light-by-light" subdiagram (see Fig. 1(f) for a sample graph) which develops the colour factors $d_F^{abcd} d_F^{abcd}/N_A$ and $C_A^2 T_F n_l$. Note that these contributions are not connected to iterations and are thus already present in QED (i.e. for $C_A = 0$, $d_F^{abcd} = 1$, $N_A = 1$ and $T_F = 1$).

Since we use non-relativistic QCD as a starting point for the evaluation of the Feynman diagrams the momentum transfer between the quark and the anti-quark represents the only relevant scale in the problem. Thus all integrals can be mapped to the two-point functions which are shown in Fig. 2 in diagrammatical form. Next to purely massless lines originating from the gluon, ghost and light-quark propagators also static lines from the heavy quarks are present. The one- and two-loop diagrams have been extensively studied in Ref. [37–39]. As far as the three-loop diagrams are concerned one can perform a partial fractioning in those cases where three static lines meet at a vertex. This leads to many different three-loop graphs involving, however, at most three static lines. Thus any resulting integral is labeled by twelve indices one of which corresponds to an irreducible numerator.

Altogether we have to consider about 70 000 integrals (allowing for a general QCD gauge parameter ξ) which can all be mapped to one of the diagrams shown in Fig. 3. Thereby the linear propagators can appear in two variants: either in the form $(-v \cdot k - i0)$ or $(-v \cdot k + i0)$. If the loop momenta, k, l and r, in the upper row of Fig. 3 are chosen as the momenta of the three upper lines, then the first diagram appears in two ways: either with the product

$$(-v \cdot k - i0)^{-a_9} (-v \cdot l - i0)^{-a_{10}} (-v \cdot r - i0)^{-a_{11}},$$

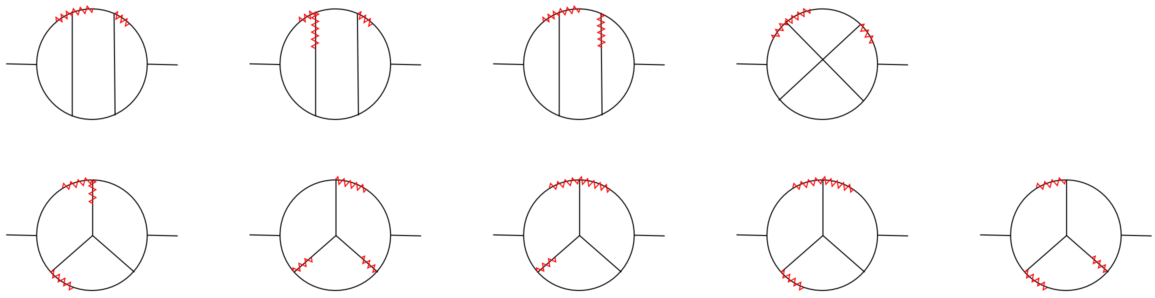

Figure 3: Three-loop diagrams of "ladder" (first three diagrams), "non-planar" (forth diagram in upper row) and "mercedes" type (lower row) which have to be considered for the fermionic part of a_3.

or with the product

$$(-v \cdot k + i0)^{-a_9}(-v \cdot l - i0)^{-a_{10}}(-v \cdot r - i0)^{-a_{11}}.$$

The second diagram appears with similar propagators where the momenta $\{k, l, r\}$ (in the first variant with $-i0$ in all three terms) are replaced by $\{k, k-l, r\}$. The third diagram in the upper row of Fig. 3 corresponds to $\{k, l, l-r\}$ and the fourth one to $\{k, l, r\}$. In the case of the "mercedes" type diagrams in the lower row of Fig. 3 one chooses the loop momenta k, l and r as the momenta of the three lower lines. Then the five diagrams appear with static propagators of the form $(-v \cdot k - i0)$ with momenta $\{k, k-r, l\}$, $\{r, k-l, r-l\}$, $\{k, r, k-l\}$, $\{k, r, l\}$, $\{k, r-l, l\}$, respectively.

For the calculation of the diagrams we proceed in the following way: They are generated with `QGRAF` [40] and further processed with `q2e` and `exp` [41, 42] where a mapping to the diagrams of Fig. 2 is achieved. In a next step the reduction of the integrals is performed with the program package `FIRE` [43] which implements a combination of the Laporta [44] and the Gröbner algorithm (see, e.g., Ref. [45]). This leads us to about 100 master integrals which have to be evaluated in an expansion in ϵ with the help of the Mellin-Barnes technique. Non trivial examples are discussed in Refs. [19, 20] where also explicit results are given. We managed to compute all but four coefficients of the ϵ expansion analytically. As a crucial tool providing very important numerical cross checks of the analytical results we applied the program `FIESTA` [46] which is a convenient and efficient implementation of the sector decomposition algorithm. Finally, let us mention that we evaluate the colour factors with the help of the program `color` [47].

In our calculation we allowed for a general gauge parameter ξ in the gluon propagator and checked that ξ drops out in the final result. This constitutes a strong check on the correctness of our result.

In order to obtain a finite result one has to renormalize the strong coupling which we perform within the $\overline{\text{MS}}$ scheme. The corresponding renormalization constant can, e.g., be found in Ref. [36].

3 Results

Let us in a first step present the results for the one- and two-loop coefficients including higher orders in ϵ since these terms are needed for the renormalization procedure. We obtain

$$
\begin{aligned}
a_1 &= \frac{31}{9}C_A - \frac{20}{9}T_F n_l + \epsilon\left[\left(\frac{188}{27} - \frac{11\pi^2}{36}\right)C_A + \left(-\frac{112}{27} + \frac{\pi^2}{9}\right)T_F n_l\right] \\
&\quad + \epsilon^2\left[\left(\frac{1132}{81} - \frac{31\pi^2}{108} - \frac{77\zeta(3)}{9}\right)C_A + \left(-\frac{656}{81} + \frac{5\pi^2}{27} + \frac{28\zeta(3)}{9}\right)T_F n_l\right], \\
a_2 &= \left(\frac{4343}{162} + 4\pi^2 - \frac{\pi^4}{4} + \frac{22}{3}\zeta(3)\right)C_A^2 - \left(\frac{1798}{81} + \frac{56}{3}\zeta(3)\right)C_A T_F n_l \\
&\quad - \left(\frac{55}{3} - 16\zeta(3)\right)C_F T_F n_l + \left(\frac{20}{9}T_F n_l\right)^2 + \epsilon\left[\left(\frac{51637}{972} - \frac{1759\pi^2}{81} + \frac{31\pi^4}{10}\right.\right. \\
&\quad \left. - \frac{220\zeta(3)}{9} - \pi^4\ln 2\right)C_A^2 + \left(-\frac{11665}{243} + \frac{217\pi^2}{81} - \frac{2\pi^4}{3} - \frac{4\zeta(3)}{9}\right)C_A T_F n_l \\
&\quad \left. + \left(-\frac{1711}{18} + \frac{\pi^2}{3} + \frac{4\pi^4}{15} + \frac{152\zeta(3)}{3}\right)C_F T_F n_l + \left(\frac{4480}{243} - \frac{40\pi^2}{81}\right)T_F^2 n_l^2\right],
\end{aligned}
\tag{4}
$$

where the one- and two-loop results (in the limit $\epsilon \to 0$) can be found in Refs. [3, 4] and [5–8], respectively. In Eq. (4) ζ is Riemann's zeta function, with the value $\zeta(3) = 1.202057\ldots$.

The three-loop result can be cast in the form

$$
a_3 = a_3^{(3)} n_l^3 + a_3^{(2)} n_l^2 + a_3^{(1)} n_l + a_3^{(0)}\,, \tag{5}
$$

where the first three coefficients on the right-hand side read

$$
\begin{aligned}
a_3^{(3)} &= -\left(\frac{20}{9}\right)^3 T_F^3\,, \\
a_3^{(2)} &= \left(\frac{12541}{243} + \frac{368\zeta(3)}{3} + \frac{64\pi^4}{135}\right)C_A T_F^2 + \left(\frac{14002}{81} - \frac{416\zeta(3)}{3}\right)C_F T_F^2\,, \\
a_3^{(1)} &= (-709.717)\,C_A^2 T_F + \left(-\frac{71281}{162} + 264\zeta(3) + 80\zeta(5)\right)C_A C_F T_F \\
&\quad + \left(\frac{286}{9} + \frac{296\zeta(3)}{3} - 160\zeta(5)\right)C_F^2 T_F + (-56.83(1))\,\frac{d_F^{abcd} d_F^{abcd}}{N_A}\,.
\end{aligned}
\tag{6}
$$

where the $SU(N_c)$ colour factors are given by

$$
C_A = N_c\,, \quad C_F = \frac{N_c^2 - 1}{2N_c}\,, \quad T_F = \frac{1}{2}\,, \quad \frac{d_F^{abcd} d_F^{abcd}}{N_A} = \frac{18 - 6N_c^2 + N_c^4}{96 N_c^2}\,. \tag{7}
$$

n_l	$\alpha_s^{(n_l)}$	1 loop	2 loop	3 loop
3	0.40	0.2228	0.2723	$32.25 \cdot 10^{-6} a_3^{(0)} - 0.2655$
4	0.25	0.1172	0.08354	$7.874 \cdot 10^{-6} a_3^{(0)} - 0.08088$
5	0.15	0.05703	0.02220	$1.701 \cdot 10^{-6} a_3^{(0)} - 0.02036$

Table 1: Radiative corrections to the potential $V(|\vec{q}\,|)$ where the tree-level result is normalized to 1 (cf. Eq. (8)).

In Eq. (6) only the coefficient of $d_F^{abcd} d_F^{abcd}$ is affected by the limited numerical precision of the four coefficients only known numerically which is indicated by the number in round brackets.

We are now in the position to briefly discuss the numerical effect of the new corrections. Inserting the results for a_1, a_2 and a_3 in Eq. (1) it takes the form

$$\begin{aligned} V(|\vec{q}\,|) &= -\frac{4\pi C_F \alpha_s(|\vec{q}\,|)}{\vec{q}^{\,2}} \Bigg[1 + \frac{\alpha_s}{\pi} (2.5833 - 0.2778 n_l) \\ &\quad + \left(\frac{\alpha_s}{\pi}\right)^2 \left(28.5468 - 4.1471 n_l + 0.0772 n_l^2\right) \\ &\quad + \left(\frac{\alpha_s}{\pi}\right)^3 \left(\frac{a_3^{(0)}}{4^3} - 51.4048 n_l + 2.9061 n_l^2 - 0.0214 n_l^3\right) + \cdots \Bigg], \end{aligned} \tag{8}$$

where the ellipses denote higher order terms and $\mu^2 = \vec{q}^{\,2}$ has been chosen in order to suppress the infrared logarithm. From Eq. (8) one observes that both at one- and two-loop order the linear n_l term is negative and leads to a screening of the (positive) non-n_l contribution by an amount of about 50% for $n_l = 5$. Also at three-loop order the linear n_l term is negative and has a sizeable coefficient. Both for a_2 and a_3 the n_l^2 contribution is small; the same is true for the n_l^3 term of a_3.

In Tab. 1 we present the one-, two- and three-loop results from the square bracket of Eq. (8) and choose n_l according to the charm, bottom and top quark case. In the second column we also provide the numerical value of α_s corresponding to the soft scale where $\mu \approx m_q \alpha_s$ (and m_q is the heavy quark mass). It is interesting to note that the three-loop corrections computed in this paper lead to corrections which are of the same order of magnitude as the two-loop corrections, however, with a different sign. In fact, one obtains corrections of about −27%, −8% and −2% for charm, bottom and top quarks, respectively. Furthermore, let us mention that the unknown constant has to be of the order 10^4 (and positive) in order to significantly reduce the size of the three-loop corrections.

Let us now compare our explicit calculation with the predictions based on Padé approximation. In Refs. [9] and [10] one can find for $a_3/4^3$ the results $\{313, 250, 193, 142, 97.5, 60.1, 30.5\}$ and $\{292, 227, 168, 116, 72, 37, 12\}$, respectively, where the entries in the list correspond to $n_l = 0, \ldots, n_l = 6$. A fit to a cubic polynomial in

n_l leads to $a_3/4^3 \approx 380.9 - 70.42 n_l + 2.34 n_l^2 + 0.08 n_l^3$ and $a_3/4^3 \approx 362.0 - 72.17 n_l + 2.00 n_l^2 + 0.17 n_l^3$, respectively. The comparison to Eq. (8) shows that the coefficients have the correct sign (except the one of n_l^3 which is, however, close to zero) and the correct order of magnitude. Let us nevertheless mention that the (numerically big) coefficient of the linear n_l term deviates by about 50%.

Finally we want to specify our result for $V(|\vec{q}\,|)$ to QED which describes the potential of two heavy leptons in the presence of n_l massless leptons. Substituting for the colour factors $C_A = 0$, $C_F = 1$, $T_F = 1$, $d_F^{abcd} = 1$ and $N_A = 1$ we obtain

$$
\begin{aligned}
V_{\rm QED}(|\vec{q}\,|) &= -\frac{4\pi\bar{\alpha}}{\vec{q}^{\,2}}\Bigg[1 + \frac{\bar{\alpha}}{\pi}\left(-0.5556 n_l\right) + \left(\frac{\bar{\alpha}}{\pi}\right)^2 \left(0.05622 n_l + 0.3086 n_l^2\right) \\
&\quad + \left(\frac{\bar{\alpha}}{\pi}\right)^3 \left(-1.131 n_l + 0.09655 n_l^2 - 0.1715 n_l^3\right) + \cdots\Bigg] \\
&= -\frac{4\pi\bar{\alpha}}{\vec{q}^{\,2}}\left[1 - 0.5556\,\frac{\bar{\alpha}}{\pi} + 0.3649\left(\frac{\bar{\alpha}}{\pi}\right)^2 - 1.206\left(\frac{\bar{\alpha}}{\pi}\right)^3 + \cdots\right], \qquad (9)
\end{aligned}
$$

where $\bar{\alpha} = \bar{\alpha}(\vec{q}^{\,2})$ is the QED coupling in the $\overline{\rm MS}$ scheme and after the second equality sign $n_l = 1$ has been chosen. This corresponds to a bound state of a muon and an anti-muon in the presence of a massless electron pair. The coefficients in Eq. (9) are significantly smaller as in the case of QCD which results in corrections of the order 10^{-8} from the three-loop term.

The terms in Eq. (9) originate from corrections to the photon propagator plus the "light-by-light"-like diagrams as in Fig. 1(f). Thus for $n_l = 1$ $V_{\rm QED}$ can be written in the form

$$
V_{\rm QED}(|\vec{q}\,|) = -\frac{4\pi}{\vec{q}^{\,2}}\frac{\alpha}{1 + \Pi(\vec{q}^{\,2})}\left[1 + \left(\frac{\alpha}{\pi}\right)^3 n_l\,(-0.888) + \cdots\right], \qquad (10)
$$

where the photon polarization function is given by

$$
\begin{aligned}
\Pi(\vec{q}^{\,2}) &= \frac{\alpha}{\pi}\left(\frac{5}{9} - \frac{L_m}{3}\right) + \left(\frac{\alpha}{\pi}\right)^2\left(\frac{5}{24} - \zeta(3) - \frac{L_m}{4}\right) + \left(\frac{\alpha}{\pi}\right)^3\Bigg[-\frac{1703}{1728} - \frac{23}{12}\zeta(2) \\
&\quad + 2\zeta(2)\ln 2 - \frac{173}{288}\zeta(3) + \frac{5}{2}\zeta(5) + \left(\frac{47}{96} - \frac{1}{3}\zeta(3)\right)L_m - \frac{L_m^2}{24}\Bigg], \qquad (11)
\end{aligned}
$$

with $\zeta(5) = 1.036927\ldots$ and $L_m = \ln \vec{q}^{\,2}/m_e^2$ where m_e is the electron mass. In Eqs. (10) and (11) we have used the fine structure constant α. The three-loop relation to $\bar{\alpha}$ can be found in Ref. [48].

4 Conclusion and outlook

In this letter we report about the calculation of the fermionic corrections to the static potential of a quark and an anti-quark. All occurring integrals are reduced to about 100 master integrals with the help of the program `FIRE`. The main result can be found in Eqs. (6) where the three-loop coefficients are given for each occurring colour structure. The numerical corrections of the new three-loop terms are quite sizeable when applied to the system of two charm, bottom or top quarks. However, for a definite conclusion one has to wait for the n_l independent three-loop coefficient $a_3^{(0)}$.

The calculation of $a_3^{(0)}$ is currently in progress. We do not expect any conceptual problems. However, significantly more Feynman diagrams contribute which leads to many new graphs in addition to those shown in Fig. 3. As a consequence also more master integrals have to be evaluated.

Acknowledgements

We would like to thank Alexander Penin for many useful discussions and communications. We also thank York Schröder for many interesting discussions at the early stage of the project. We thank Yuichiro Kiyo, Hans Kühn, Alexander Penin and York Schröder for useful comments to the manuscript. M.S. thanks Luminita Mihaila, Jan Piclum and Jos Vermaseren for discussions on colour factors. This work was supported by RFBR, grant 08-02-01451 and by the DFG through SFB/TR 9.

References

[1] N. Brambilla *et al.* [Quarkonium Working Group], arXiv:hep-ph/0412158.

[2] A. Vairo, AIP Conf. Proc. **964** (2007) 102 [arXiv:0709.3341 [hep-ph]].

[3] W. Fischler, Nucl. Phys. B **129** (1977) 157.

[4] A. Billoire, Phys. Lett. B **92** (1980) 343.

[5] M. Peter, Phys. Rev. Lett. **78** (1997) 602 [arXiv:hep-ph/9610209].

[6] M. Peter, Nucl. Phys. B **501** (1997) 471 [arXiv:hep-ph/9702245].

[7] Y. Schroder, Phys. Lett. B **447** (1999) 321 [arXiv:hep-ph/9812205].

[8] B. A. Kniehl, A. A. Penin, M. Steinhauser and V. A. Smirnov, Phys. Rev. D **65** (2002) 091503 [arXiv:hep-ph/0106135].

[9] F. A. Chishtie and V. Elias, Phys. Lett. B **521** (2001) 434 [arXiv:hep-ph/0107052].

[10] A. Pineda, JHEP **0106** (2001) 022 [arXiv:hep-ph/0105008].

[11] T. Appelquist, M. Dine and I. J. Muzinich, Phys. Rev. D **17** (1978) 2074.

[12] N. Brambilla, A. Pineda, J. Soto and A. Vairo, Phys. Rev. D **60** (1999) 091502 [arXiv:hep-ph/9903355].

[13] N. Brambilla, A. Pineda, J. Soto and A. Vairo, Nucl. Phys. B **566** (2000) 275 [arXiv:hep-ph/9907240].

[14] B. A. Kniehl and A. A. Penin, Nucl. Phys. B **563** (1999) 200 [arXiv:hep-ph/9907489].

[15] B. A. Kniehl, A. A. Penin, V. A. Smirnov and M. Steinhauser, Nucl. Phys. B **635** (2002) 357 [arXiv:hep-ph/0203166].

[16] A. A. Penin and M. Steinhauser, Phys. Lett. B **538** (2002) 335 [arXiv:hep-ph/0204290].

[17] A. Pineda and J. Soto, Phys. Lett. B **495** (2000) 323 [arXiv:hep-ph/0007197].

[18] N. Brambilla, X. Garcia i Tormo, J. Soto and A. Vairo, Phys. Lett. B **647** (2007) 185 [arXiv:hep-ph/0610143].

[19] A. V. Smirnov, V. A. Smirnov and M. Steinhauser, PoS **RADCOR2007** (2007) 024 [arXiv:0805.1871 [hep-ph]].

[20] A. V. Smirnov, V. A. Smirnov and M. Steinhauser, arXiv:0807.0365 [hep-ph].

[21] M. Beneke, Y. Kiyo, A. Penin and K. Schuller, arXiv:0710.4236 [hep-ph].

[22] G. S. Bali, Phys. Lett. B **460** (1999) 170 [arXiv:hep-ph/9905387].

[23] S. Necco and R. Sommer, Phys. Lett. B **523** (2001) 135 [arXiv:hep-ph/0109093].

[24] A. Pineda, J. Phys. G **29** (2003) 371 [arXiv:hep-ph/0208031].

[25] Y. Sumino, Phys. Rev. D **76** (2007) 114009 [arXiv:hep-ph/0505034].

[26] C. T. H. Davies, I. D. Kendall, G. P. Lepage, C. McNeile, J. Shigemitsu and H. Trottier [HPQCD Collaboration], arXiv:0807.1687 [hep-lat].

[27] K. Maltman, D. Leinweber, P. Moran and A. Sternbeck, arXiv:0807.2020 [hep-lat].

[28] S. N. Gupta and S. F. Radford, Phys. Rev. D **25** (1982) 3430.

[29] J. T. Pantaleone, S. H. H. Tye and Y. J. Ng, Phys. Rev. D **33** (1986) 777.

[30] S. Titard and F. J. Yndurain, Phys. Rev. D **49** (1994) 6007 [arXiv:hep-ph/9310236].

[31] A. V. Manohar, Phys. Rev. D **56** (1997) 230 [arXiv:hep-ph/9701294].

[32] A. Pineda and J. Soto, Phys. Rev. D **58** (1998) 114011 [arXiv:hep-ph/9802365].

[33] A. V. Manohar and I. W. Stewart, Phys. Rev. D **62** (2000) 074015 [arXiv:hep-ph/0003032].

[34] M. Melles, Phys. Rev. D **62** (2000) 074019 [arXiv:hep-ph/0001295].

[35] B. A. Kniehl, A. A. Penin, Y. Schroder, V. A. Smirnov and M. Steinhauser, Phys. Lett. B **607** (2005) 96 [arXiv:hep-ph/0412083].

[36] K. G. Chetyrkin, Nucl. Phys. B **710** (2005) 499 [arXiv:hep-ph/0405193].

[37] M. Peter, "Schwere Quark-Antiquark-Systeme und störungstheoretische QCD", PhD thesis (1997), University of Karlsruhe.

[38] Y. Schroder, "The static potential in QCD", PhD thesis (1999), University of Hamburg.

[39] V. A. Smirnov and M. Steinhauser, Nucl. Phys. B **672** (2003) 199 [arXiv:hep-ph/0307088].

[40] P. Nogueira, J. Comput. Phys. **105** (1993) 279.

[41] R. Harlander, T. Seidensticker and M. Steinhauser, Phys. Lett. B **426** (1998) 125 [hep-ph/9712228].

[42] T. Seidensticker, hep-ph/9905298.

[43] A. V. Smirnov, arXiv:0807.3243 [hep-ph].

[44] S. Laporta and E. Remiddi, Phys. Lett. B **379** (1996) 283 [arXiv:hep-ph/9602417].

[45] B. Buchberger and F. Winkler (eds.), *Gröbner Bases and Applications*, Cambridge University Press, 1998.

[46] A. V. Smirnov and M. N. Tentyukov, arXiv:0807.4129 [hep-ph].

[47] T. van Ritbergen, A. N. Schellekens and J. A. M. Vermaseren, Int. J. Mod. Phys. A **14** (1999) 41 [arXiv:hep-ph/9802376].

[48] D. J. Broadhurst, Z. Phys. C **54** (1992) 599.